UDK: 662.767.3:519.673
COSATI: 20-12, 13-04, 21-04

Stress and Strain States in the Material of the Stressed Toroidal Container for Liquefied Petroleum Gas

Vladan Veličković, MSc (Eng)[1)]

Analytical methods for the calculation of stress and strain states can be applied with satisfactory accuracy in a great number of practical technical problems (see, for example, Ref. [1, 2])
Because of an untypical shape of the cross section of the LM-630 toroidal container for liquefied petroleum gas as well as the existence of the sources of the stress concentration, it was practically impossible to apply analytical methods for the calculation of the stress and strain states in the walls of the container. This fact was a reason to apply the structural analysis.
The paper, along with theoretical considerations, discusses the most important steps as well as the main results of the numerical calculation of the components of the stress and strain states of the LM-630 toroidal container. The obtained results demonstrate that the container satisfies the design requirements regarding its strength.

Key words: **stress state, strain state, structural analysis, toroidal container, liquefied petroleum gas.**

Introduction

THE use of liquid petroleum gas (LPG) as a fuel source in motor vehicles is steadily increasing. LPG tanks are pressure vessels, which can normally be considered as thin shells. The shapes of pressure vessels that have been studied extensively over the years are mostly cylindrical, spherical and conical. Toroidal vessels have received lesser attention, largely due to their greater geometric complexity. The mechanical properties which are of interest for toroidal LPG containers are the static behavior under internal pressure and collapse loads.

Most research work on toroidal shells or tanks has been carried out for circular or elliptical cross-sections. Stress and vibration analyses of toroidal shells of elliptical cross-section were conducted, respectively, by Sutcliffe [3] and by Yamada et al. [4]. Galetly [5] and Combesture and Galletly [6], respectively, have determined results for elastic and plastic buckling pressures of toroidal shells with circular and elliptic cross-sections.

The "Lifam – M" firm from Stara Pazova (Serbia) designs and manufactures toroidal containers for liquefied petroleum gas which is used in the propulsion system of motor vehicles.

If a manufacturer wants to obtain, from international authorized officials, a certificate for the production of containers for the aforementioned purpose, he must prove that the product satisfies relevant technical requirements [7] based on the current knowledge in this area of science.

A part of these technical requirements (Annex 10 of the document [7]) concerns the strength or, in other words, the carrying capacity of the container structure. The fulfillment of these requirements can be checked by the inspection of the stress and/or strain state of the structure under the action of corresponding levels of the internal pressure (the test pressure and the bursting pressure).

The necessary calculations were made in the Military Technical Institute and the partial results are presented in reference [8].

The ratio of the wall thickness and other dimensions is such that this toroidal container can be regarded as a shell and the shape of the container is the shell in the form of the surface of revolution.

The theoretical bases of the calculation of the stress state in the wall points of such shells are given, for example, in [9] and [10], and the expressions for the calculation of the stress state in the wall points of the circular torus submitted to the action of the internal pressure can be found, for example, in [9] and [11].

However, the initial shape of the cross section of the LM-630 toroidal container considerably differed from the circle. Besides that, it was estimated that the toroidal container fitting would be the source of the significant stress concentration.

Because of the cited reasons, it was not possible to calculate stress and strain state components using analytical methods, but, by the use of a commercial software, the structural analyses were performed.

At first, the structural analysis of the theoretical circular torus submitted to the action of the uniform internal pressure was performed in order to compare the obtained results with the analytically obtained solutions. When the excellent agreement was seen, the calculation of the LM-630 started.

In this paper, the following aspects of the structural analysis of the LM-630 toroidal container are discussed:

- the most important steps in preparing the input data (geometry, material characteristics, load),
- basic problems connected with satisfying technical requirements, and
- the most important results of the final structural analysis.

[1)] Military Technical Institute (VTI), Ratka Resanovića 1, 11132 Belgrade, SERBIA

In this work, the stress analyses of the nonlinear material and the geometrical properties are carried out for a toroidal container with a given cross-section. The analyses are made using the finite element method (FEM). The computation procedure is validated by comparing the FE results with the analytical results.

The theoretical basis of the calculation of the stress state components in the shells in the form of the surface of revolution

A toroidal container the wall thickness of which is small in comparison with its other dimensions can be considered as a shell in the form of the surface of revolution (see Ref. [12]).

Such shells find extensive application in various kinds of pressure vessels. The surface of revolution is obtained by the rotation of a plane curve around the axis lying in the curve plane. This curve is called the meridian and its plane is a meridian plane. A line representing the intersection of the surface of revolution and the plane normal to the meridian plane is called the parallel circle.

An element of such a shell is cut out by two adjacent meridians and two parallel circles, as shown in Fig.1. The position of the meridian is defined by an angle θ, and the position of the parallel circle is defined by the angle φ, mode by the normal to the surface and the rotation axis. The meridian plane and the plane perpendicular to the meridian are the planes of the principal curvature at a point of the surface of revolution, and the corresponding curvature radii are denoted by r_1 and r_2, respectively. The radius of the parallel circle is denoted by r_0 so that the length of the sides of the elements are $r_1 d\varphi$ and $r_0 d\theta = r_2 \sin\varphi d\theta$. The surface area of the element is then $r_1 r_0 d\theta d\varphi = r_1 r_2 \sin\varphi d\varphi d\theta$.

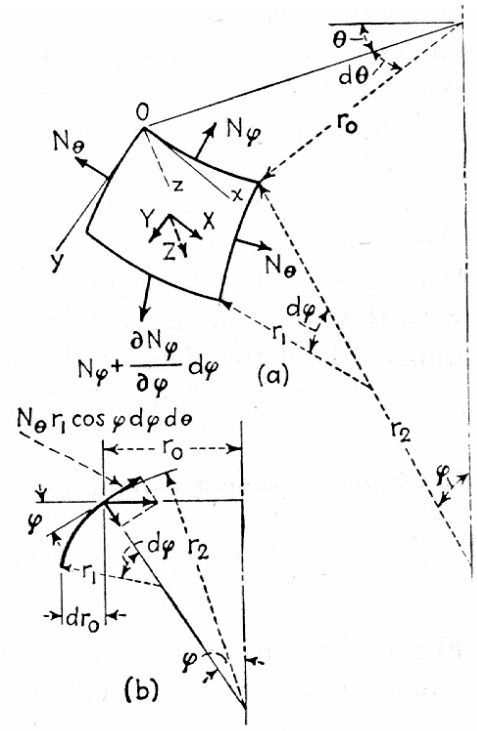

Figure 1. Stress state components of the element of the shell in the form of the surface of revolution

From the assumed symmetry of loading and deformation it can be concluded that there will be no shearing forces acting on the sides of the element. The magnitudes of the normal forces per unit length which act on the element are denoted by N_φ and N_θ, as shown in the figure. The intensity of the external load per unit area, which acts in the meridian plane, in the case of symmetry is resolved in two components Y and Z parallel to the coordinate axes. The components of the external force acting on the element are obtained by multiplying the components Y and Z with the corresponding area of the element.

The first equation of the force equilibrium of the considered element is obtained by summing up the projections of the forces in the z direction. The forces acting on the upper and lower sides of the element have a resultant in the z direction equal to

$$N_\varphi r_0 d\theta d\varphi \tag{1}$$

The forces acting on the lateral sides of the element and having the resultant $N_\theta r_1 d\theta d\varphi$ in the radial direction of the parallel circle give a component in the z direction of the magnitude

$$N_\theta r_1 \sin\varphi d\theta d\varphi \tag{2}$$

The external load acting on the element has in the same direction a component

$$Z r_0 r_1 d\theta d\varphi \tag{3}$$

Summing up the forces (1), (2) and (3) the following equation of equilibrium is obtained

$$N_\varphi r_0 + N_\theta r_1 \sin\varphi + Z r_0 r_1 = 0 \tag{4}$$

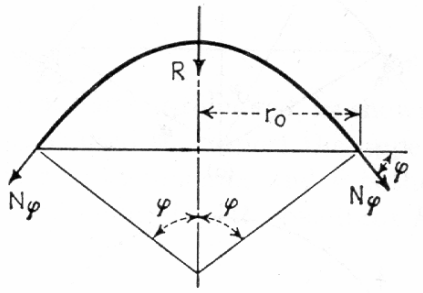

Figure 2. Equilibrium of the forces applied to the part of the shell

The second equation of the equilibrium of the forces can be obtained by considering the equilibrium of the forces applied to the part of the shell above the parallel circle defined by the angle φ (see Fig.2). If the resultant of the total load on that part of the shell is denoted by R, the equation of equilibrium is

$$2\pi r_0 N_\varphi \sin\varphi + R = 0 \tag{5}$$

If Eq. (4) is divided by $r_1 r_o$, it can be written in the form (see Ref. [12])

$$\frac{N_\varphi}{r_1} + \frac{N_\theta}{r_2} = -Z \tag{6}$$

It can be seen that when N_φ is obtained from Eq. (5), the force N_θ can be calculated from Eq. (6). Hence the problem of membrane stresses can be readily solved in each

particular case. The solution requires to determine the radii of the principal curvature. The general expressions for their calculation are given in [10, p.216].

In the particular case we are interested in a toroidal shell which is obtained by rotating a circle of the radius a around the vertical axis (Fig.3). The axis is at the distance b from the center of the circle.

The point A is on the parallel circle the radius of which is $r_0 = b + a\sin\varphi$, and the radii of the principal curvatures in this point are

$$r_1 = a \wedge r_2 = \frac{r_0}{\sin\varphi} = a + \frac{b}{\sin\varphi}$$

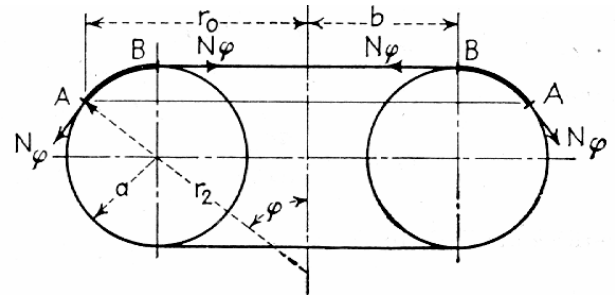

Figure 3. Circular torus

The forces N_φ are obtained by considering the equilibrium of the ring-shaped portion of the shell represented in Fig.3 by the bold line AB. Since the forces N_φ along the parallel circle BB are horizontal, we need to consider only the forces N_φ along the circle AA and the external forces acting on the ring when discussing the equilibrium in the vertical direction.

Assuming that the shell is submitted to the action of the uniform internal pressure p, Eq. (5) obtains the form

$$2\pi r_0 N_\varphi \sin\varphi = \pi p\left(r_0^2 - b^2\right)$$

from which

$$N_\varphi = \frac{p\left(r_0^2 - b^2\right)}{2r_0\sin\varphi} = \frac{pa\left(r_0 + b\right)}{2r_0} \tag{7}$$

Substituting this expression in Eq. (6), it is obtained

$$N_\theta = \frac{pr_2\left(r_0 - b\right)}{2r_0} = \frac{pa}{2} \tag{8}$$

For the shell with a constant wall thicknessδ, the corresponding normal stresses are

$$\sigma_\varphi = \frac{N_\varphi}{\delta} = \frac{pa}{2\delta}\cdot\frac{r_0 + b}{r_0} \wedge \sigma_\theta = \frac{N_\theta}{\delta} = \frac{pa}{2\delta} \tag{9}$$

However, if in a thin vessel there are abrupt changes in the wall thickness or the curvatures, such occurrences will cause additional bending and shear stresses which are superposed upon the membrane stresses.

The expression of displacement of the shell in the radial direction is given in [11, p.454]

$$\Delta r_0 = \frac{p\cdot a}{2E\cdot\delta}\left[r_0 - \nu\left(r_0 + b\right)\right] \tag{10}$$

where E and ν denotes the modulus of elasticity and Poisson's ratio of the shell material, respectively.

Validation of computation procedure

Because of the validation of the finite element method, the comparison of the numerical and the analytical solutions is presented. For that purpose a circular toroidal vessel under internal pressure is chosen.

Analytic computation solutions

A circular toroidal vessel submitted to the action of the uniform internal pressure $p = 0.3\ \mathrm{daN/mm^2}$ was considered. The dimensions of the vessel are (see Fig.3)

$$a = 105.9\ \mathrm{mm};\quad b = 207.5\ \mathrm{mm};\quad \delta = 3.2\ \mathrm{mm}$$

and the characteristics of elasticity are

$$E = 19000\ daN/mm^2 \quad \wedge \quad \nu = 0.3$$

Introducing the aforementioned values in Eq. (10), the following expression for the shell point transversal displacements in the radial direction is obtained

$$\Delta r_0 = 0.000261\cdot\left(0.7r_0 - 62.25\right)$$

The normal stress σ_θ is constant in the entire vessel and is equal to

$$\sigma_\theta = \frac{pa}{2\delta} = \frac{0.3\cdot 105.9}{2\cdot 3.2} = 4.96\ \mathrm{daN/mm^2}$$

The expression for the calculation of the meridional stress σ_φ along certain parallel circles, which are defined by their radii r_o, is obtained from Eqs. (9)

$$\sigma_\varphi = \sigma_\theta\cdot\frac{r_0 + b}{r_0} = 4.96\cdot\frac{r_0 + 207.5}{r_0}$$

The upper and lower limits of the radius r_o are

$$r_{0\min} = b - a = 101.6\ \mathrm{mm} \quad \wedge \quad r_{0\max} = b + a = 313.4\ \mathrm{mm}$$

The values of the displacement Δr_0 and meridional stress as well as the Von Misses stress for several values of the radius r_0 are given in Table 1. The Von Misses stress is given by the expression

$$\sigma_{VM} = \sqrt{\sigma_\varphi{}^2 + \sigma_\theta{}^2 - \sigma_\varphi\sigma_\theta} \tag{11}$$

and it was used for the comparison of the analytical and numerical solutions.

Table 1. Stresses and displacements of the circular torus

r_0 (mm)	$\sigma_\varphi\ (\mathrm{daN/mm^2})$	$\sigma_{VM}\ (\mathrm{daN/mm^2})$	Δr_0 (mm)
101.6	15.09	13.32	0.002
150	11.82	10.28	0.011
200	10.11	8.75	0.020
250	9.08	7.87	0.029
300	8.39	7.31	0.039
313.4	8.24	7.19	0.041

Finite element solutions

After that, the model of the circle toroidal vessel (See Fig.3) with the same dimensions and characteristics of elasticity was prepared. The model had 3200 nodes and 3200 plate elements (CQUAD4). The loading of the vessel

was the internal pressure $p = 0.3\ \mathrm{daN/mm^2}$ and the constraints were carried out in four symmetrically placed nodes at the radius $r_0 = b = 207.5\ \mathrm{mm}$. The linear structural analysis was performed using the MSC/NASTRAN software package [13].

The distribution of the Von Misses stresses in the model elements is depicted in Fig.4, and the displacements in the radial direction are depicted in Fig.5.

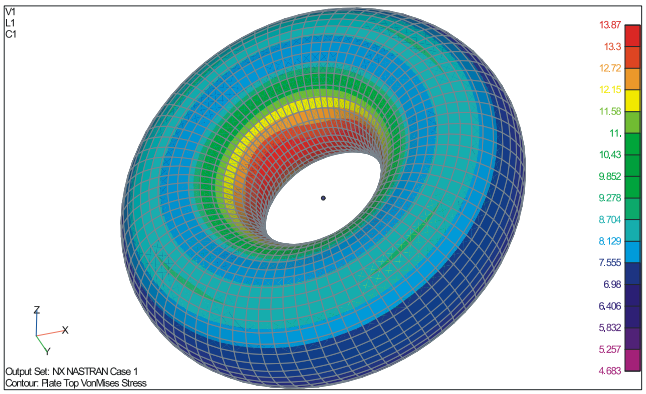

Figure 4. Von Misses stresses in the circular torus

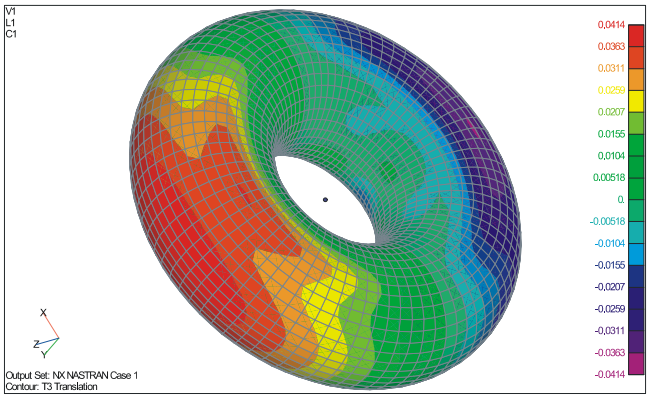

Figure 5. Radial displacements of the circular torus

The values of the Von Misses stress in the elements of the model which are sufficiently far from the constraint nodes are between $7.24\ \mathrm{daN/mm^2}$ and $13.56\ \mathrm{daN/mm^2}$ and it is difference of about 1.5% in regard to the values given in Table 1.

The values of the radial displacement are between 0.002 mm and 0.0414 mm which is an excellent agreement in regard to the values given in Table 1.

The work on the structural analysis of the LM-630 container started after excellent agreement between the analytical and numerical solutions was established.

Structural analyses of the toroidal container by FEM

The analyses are made using the finite element method. Special attention in the analyses is focused on elastic-plastic behavior of the material of the container. The nonlinear FEM program NASTRAN was used in this work for the numerical analyses. The following data are given in the next sections: geometric properties, characteristics of material, technical requirements, CAD model and finite element models and results of the analyses.

Description of the container

The Fig.6 shows the total cross section of the welded assembly of the LM – 630 toroidal container.

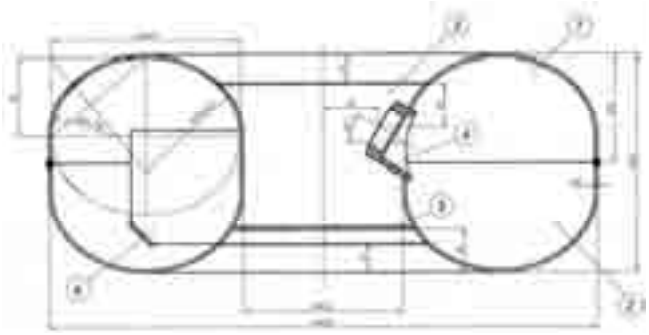

Figure 6. Welded assembly of the LM – 630 toroidal container

The Fig.7 shows the exploded view of the container with the marked main parts the names of which are given in Table 2.

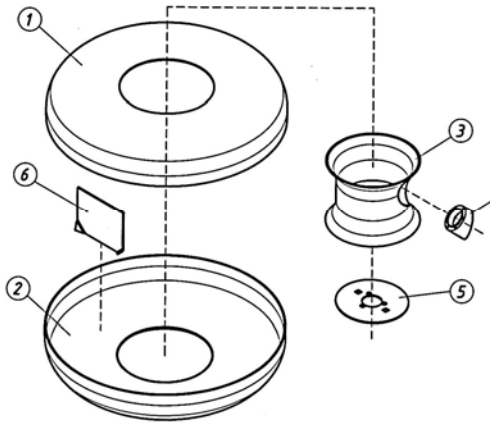

Figure 7. Exploded view of the toroidal container

Table 2. Main parts of the toroidal container

Position	Part name
1	Top sphere
2	Bottom sphere
3	Cylindrical shell
4	Toroidal container fitting
5	Marking plate
6	Barrier

All parts of the container, except fitting, are made from the 3.2 mm thick steel sheet. The material of the sheet is FeE 265 KR/EU 120-83. The fitting is made from the C20 UNI 7874 steel.

All parts are welded together making an inseparable unit. The welded container is normalized to 920°C and, after that, tested in accordance with the requirements given in [7].

Design characteristics of used material

The following mechanical characteristics for the sheet material FeE 265 KR/EU 120-83 were available:

– minimal value of the upper yield stress, $\sigma_y = 26.5\ \mathrm{daN/mm^2}$

– minimal value of the tensile strength, $\sigma_m = 41\ \mathrm{daN/mm^2}$ and

– elongation at reaching the tensile strength, $\varepsilon_m = 0.28\,\text{mm}/\text{mm} = 28\%$.

The value of the modulus of elasticity which was necessary for the structural analysis was not known. To establish an accurate value of the modulus of elasticity, a few appropriate specimens of the material were tested in the relevant laboratory of the Military Technical Institute. The obtained value was $E \approx 19000\,\text{daN}/\text{mm}^2$ and it was used in all calculations.

The paragraph 1.5.1 of Annex 10 [7] issues two values of the corrective factor (z) for the yield stress for the containers with welded parts. The paragraph issues that a reduced value of the yield stress should be used in the calculation, i.e. $\sigma_y^c = z \cdot \sigma_y$.

One or another value is used in calculations depending on the level of strictness in inspecting the welds. The detail description of the levels of inspection is described in paragraph 1.5.1, too.

The values of the corrective factor are:

– $z = 0.85$ - for less strict inspection and

– $z = 1$ - for extremely strict inspection

The application of the value $z = 0.85$ was agreed with the manufacturer because of its inspection possibilities and costs. The same corrective factor is used for the tensile strength, too.

So, the following design values were adopted for all structural analyses:

– minimum value of the upper yield stress, $\sigma_y^c = 0.85 \cdot 26.5 = 22.525\,\text{daN}/\text{mm}^2$,

– minimum value of the tensile strength, $\sigma_m^c = 0.85 \cdot 41 = 34.85\,\text{daN}/\text{mm}^2$,

– elongation at reaching the tensile strength, $\varepsilon_m = 0.28\,\text{mm}/\text{mm} = 28\%$ and

– modulus of elasticity, $E = 19000\,\text{daN}/\text{mm}^2$.

For the structural analysis [13] with nonlinear material properties, one has to know the behavior of the material up to the ultimate load, i.e. the complete stress – strain curve for the material is necessary.

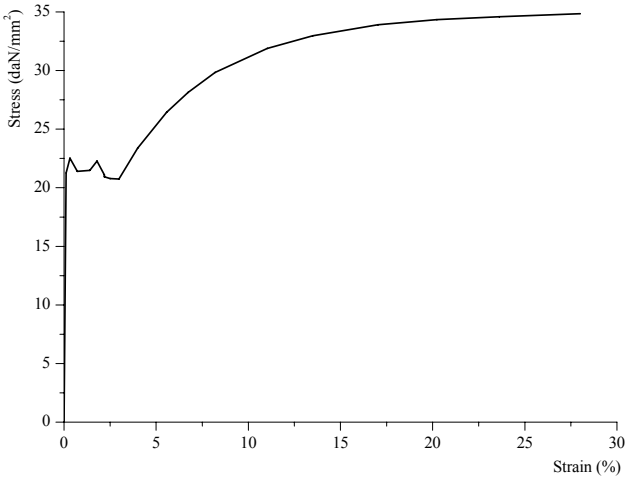

Figure 8. Design stress-strain curve for the FeE 265 KR/EU 120-83 steel

For this reason, the so-called design curve (Fig.8) for the FeE 265 KR/EU 120-83 steel was constructed on the basis of the previously defined design values of mechanical characteristics and behavior of the material registered during the tests.

From the aspect of the strain state of the container structure, it is very important to know the strain value (ε_y) that corresponds to the yield stress. As it can be seen from Fig.8 as well as from stress-strain diagrams for the majority of steels, a sharp break exists at a stress value just after reaching the proportional limit which represents the maximum stress in which strain remains directly proportional to stress. The mentioned break of the curve is shown with the first sharp peak in Fig.8. At this critical stress, material elongates considerably with no increase in stress. The stress at which this takes place is referred to as the upper yield point.

Since permanent deformations of any appreciable amount are undesirable in most structures, it is customary to adopt an arbitrary amount of permanent strain that is considered admissible for practical purposes. The value of this strain has been established by material testing engineers as $\varepsilon_p = 0.2\%$.

For practical purposes, the yield stress may be determined from the stress-strain curve by drawing a line parallel to the straight (or elastic) portion of the curve through a point representing zero stress and 0.002 strain. The yield stress is taken as the stress at the intersection of this straight line with the stress-strain curve.

The strain value that corresponds to the yield stress may be calculated on the basis of aforementioned facts and using Fig.9.

From Fig.9, it follows

$$\sigma_y = E \cdot (\varepsilon_y - \varepsilon_p) \tag{12}$$

and further

$$\varepsilon_y = \frac{\sigma_y}{E} + \varepsilon_p \tag{13}$$

With the aforementioned values of the adopted design values of mechanical characteristics, the value ε_y^c=0.3186% is obtained as the strain at the design yield stress.

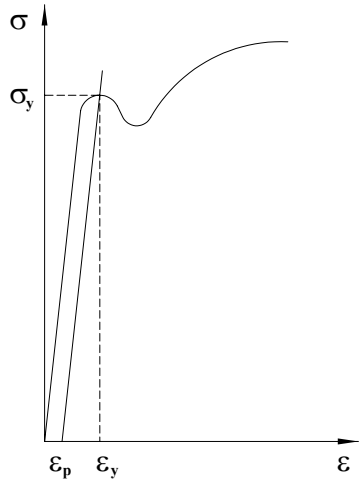

Figure 9. Yield stress and corresponding strains

Technical requirements in regard the strength of container material and structure

The technical requirements in regard to the strength of the container structure enter the scope of Annex 10 of the document [7].

These requirements issue that a container must withstand an inner hydraulic test pressure $p_h = 3000\,\text{kPa} = 0.3\,\text{daN/mm}^2$ without becoming permanently distorted (paragraphs 2.3.1 and 2.3.4 of Annex 10).

From the aspect of the structural analysis this fact means that, at this load level, the Von Misses stress in any element must not exceed a value of the design yield stress $\sigma_y^c = 22.525\,\text{daN/mm}^2$.

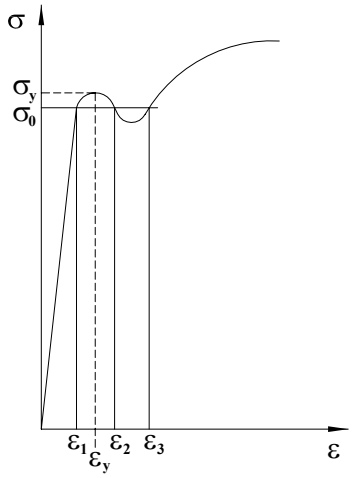

Figure 10. Different strain values for the same stress value

However, the stress value which is lower than the yield stress could exist at various strain values as it is depicted schematically in Fig.10. In this Figure only strain ε_1 is less than ε_y , but other two strain values are higher than ε_y .

Because of that, the Von Misses strain in any element has to be lower than the corresponding design strain $\varepsilon_y^c = 0.003186\,\text{mm/mm} = 0.3186\%$.

The satisfying of these conditions guarantees that permanent strain after unloading will be less than 0.2% which is considered admissible for practical purposes, as it was mentioned earlier.

Besides that, the requirements issue that the inner bursting pressure must not be less than $p_b = 2.25 \cdot p_h = 6,750\,\text{kPa} = 0.675\,\text{daN/mm}^2$ (paragraph 2.2.3.1 of Annex 10).

From the aspect of the structural analysis this fact means that, at this load level, the Von Misses stress in any element must not exceed the design tensile strength of the material $\sigma_m^c = 34.85\,\text{daN/mm}^2$. At the same time, the Von Misses strain in any element has to be lower than the elongation at the tensile strength $\varepsilon_m = 0.28\,\text{mm/mm} = 28\%$.

Description of the calculation model

The basis for the model geometry was the geometry of the container which included overall dimensions of the container and shape of the characteristic cross section.

The overall dimensions of this type of the container are:

– outer diameter $D = 630\,\text{mm}$,

– inner diameter $d = 183.5\,\text{mm}$ and

– height $H = 250\,\text{mm}$.

These overall dimensions with the finally accepted shape of the characteristic cross section are depicted in Fig.6.

The basic AutoCAD geometry data for creating the model are schematically depicted in Fig.11. The following designation is used in this Figure:

– axis of symmetry of the container (1),

– theoretic middle line of the cross section of the container (2),

– axis of container fitting (3) and

– middle line of the contour of the fitting (4).

This geometry was imported in FEMAP where all other activities were performed. The body and the fitting of the container were obtained by revolving contour 2 and line 4 about axes 1 and 3 respectively. The resulting solids were intersected and joined after the removal of excess surfaces. The transition line between the body and the fitting of the container was filleted after that.

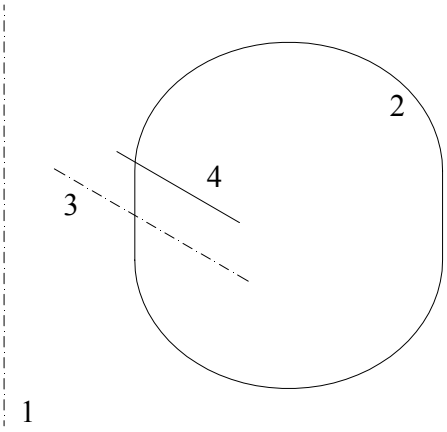

Figure 11. Basic input geometry for the model creation

After inserting the barrier, marking the plate and the cover of the fitting, the model was divided into appropriate four-sided surfaces for easy mesh generation. The resulting mesh was adjusted by minimizing the element distortion. The surface model is presented in Fig.12.

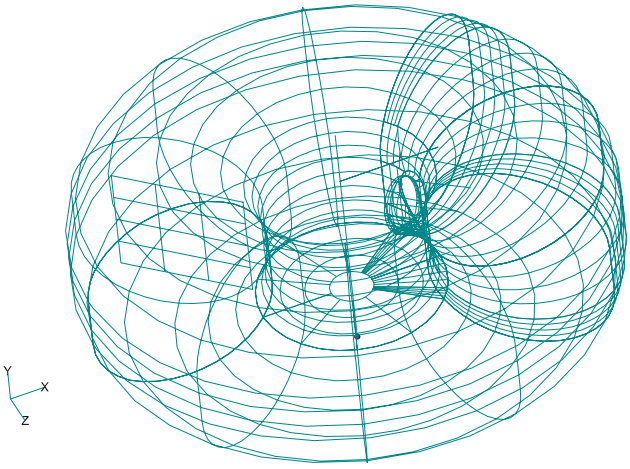

Figure 12. Surface model of the container

The next step was the creation of the properties. One isotropic material with described mechanical characteristics was used for all elements. Several properties differ on the basis of various thicknesses. The thickness of top and bottom sphere, cylindrical shell, barrier and marking plate was constant (3.2 mm) all over the container model. The exceptions were the overlapping zones of the parts where the welding was carried out as well as the fillet zone between the fitting and the cylindrical shell which had appropriate greater thicknesses. The entire container was modeled with plate elements (CQUAD4). The model had 5706 nodes and 5707 elements. The constraints were carried out by pinning the edge of the center hole of the

marking plate. The loadings of the container were corresponding internal pressures on all elements.

Basic problems connected with satisfying technical requirements

The structural analyses were performed using the MSC/NASTRAN software package [13].

The analysis for the minimal bursting pressure was performed using the MSC/NASTRAN capability of structural analysis. Also, the structural analysis, using nonlinear structural properties, was applied for the test pressure because the allowable normal stress component σ_y^c and the corresponding strain component ε_y^c were in the nonlinear part of the stress-strain curve of the material constitutive law.

The structural analysis, which uses nonlinear structural properties, was also necessary for a complete stress-strain constitutive relation graphically presented by the corresponding curve for the used material.

It was evident that the requirements for the test pressure were more severe than for the bursting pressure since the stress components and the corresponding strain components in all element points must "fall" in a very narrow zone.

Also, on the basis of some preliminary analysis, it seemed that the original shape of the cross section was not good enough. One of the reasons was that cross section had both relatively large and small radii (see Fig.13) and such a combination, as already mentioned, causes additional bending and shear stresses which are superposed upon the normal stresses in the membrane.

In addition to everything else, certain problems were expected in the region where the fitting was attached to the cylindrical shell and it was a zone of the stress concentration, as well.

Because of all the mentioned reasons, the first structural analysis was performed for the test pressure $p_h = 0.3\,\mathrm{daN/mm^2}$.

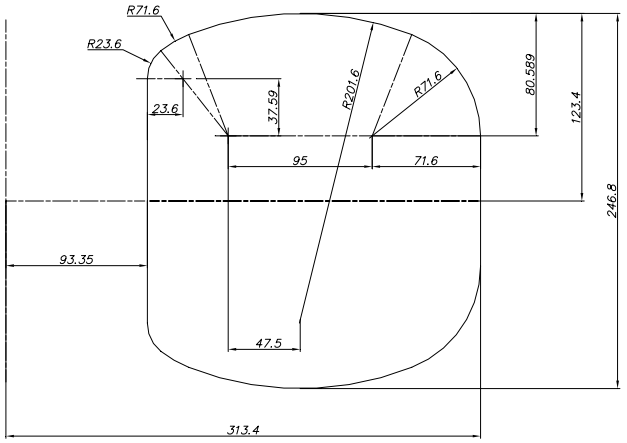

Figure 13. Theoretical measures of the original shape of the cross section of the container

But, as it was expected, the results for the original shape of the cross section of the container were not satisfactory. Both stresses and strains were considerably above their allowable values in almost all parts of the global structure of the container (top and bottom sphere, cylindrical shell,...).

This fact caused looking for an appropriate shape of the cross section. It was a difficult job because this shape had to give satisfying results regarding the stress and strain state, but it also had to enable production of the container.

A few words will be said about the fact which made the choosing of an optimal shape of the cross section so hard. In most of practical applications it is not necessary to satisfy stress and strain conditions in an entire structure.

The main reason is that the finite element model is simplified to a certain degree in regard to the real structure. Such simplifications can be the sources of stress concentration in the model and cause the occurrence of local high stresses and strains in the zones where they actually does not exist. An experienced stress engineer usually neglects the results for such zones and uses some of the classic engineering methods to calculate them.

However, for this particular case, it was required that the stresses and strains had to be bellow allowable values in all elements of the model. This requirement caused that model was made exceptionally carefully in order to minimize deviations of the model regarding the real container.

The structural analysis was repeated for various shapes of the cross section until the final shape was chosen for which the Von Misses stresses and the corresponding strains were bellow allowable values in all elements of the model. This shape of the cross section can be seen in Fig.6.

Main results of the structural analyses for the nonlinear properties of the container material

The distributions of the Von Misses stresses and strains in the main parts of the container model are shown in Figures 14 to 19 and their maximum values are given in Table 3.

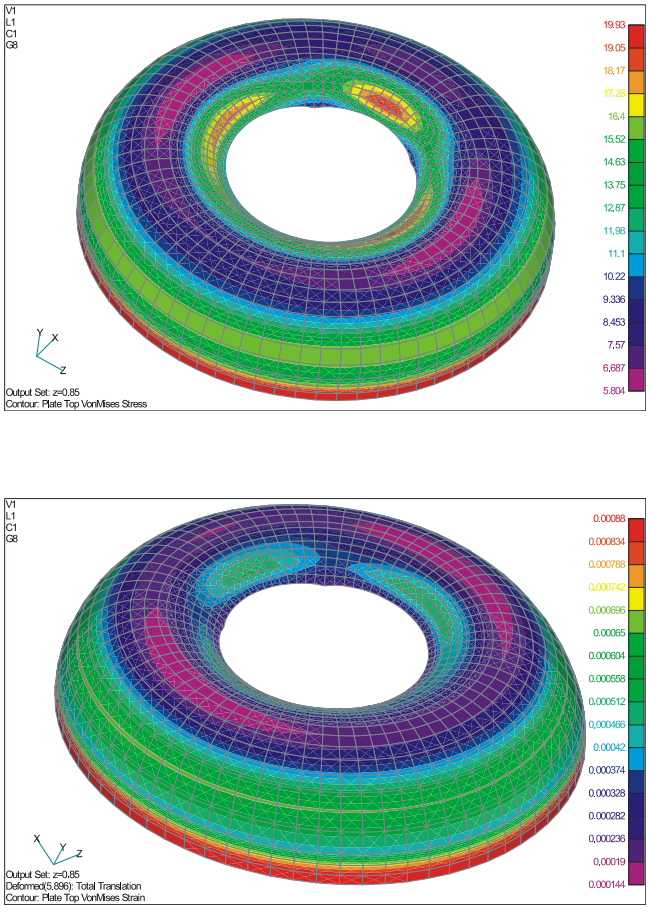

Figure 14. Distributions of the Von Misses stresses (up) and strains (down) on the top sphere

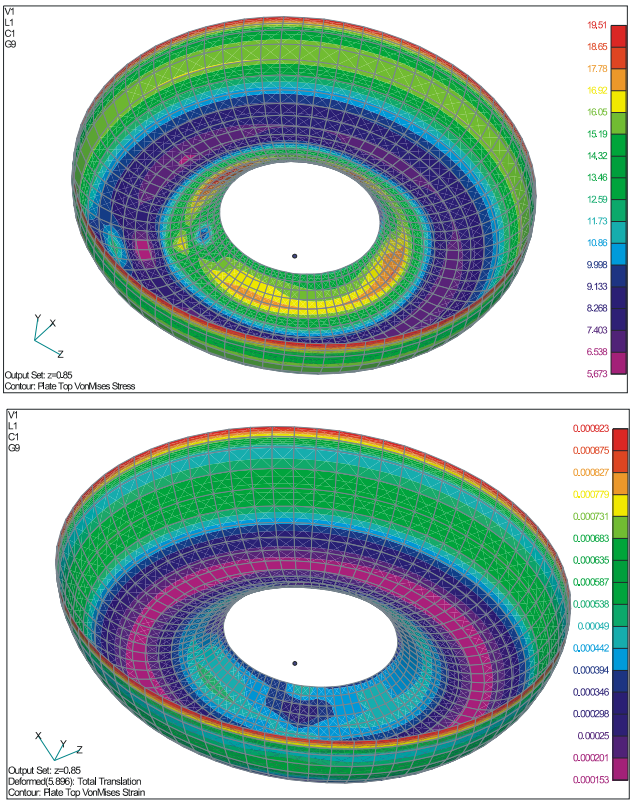

Figure 15. Distributions of the Von Misses stresses (up) and strains (down) on the bottom sphere

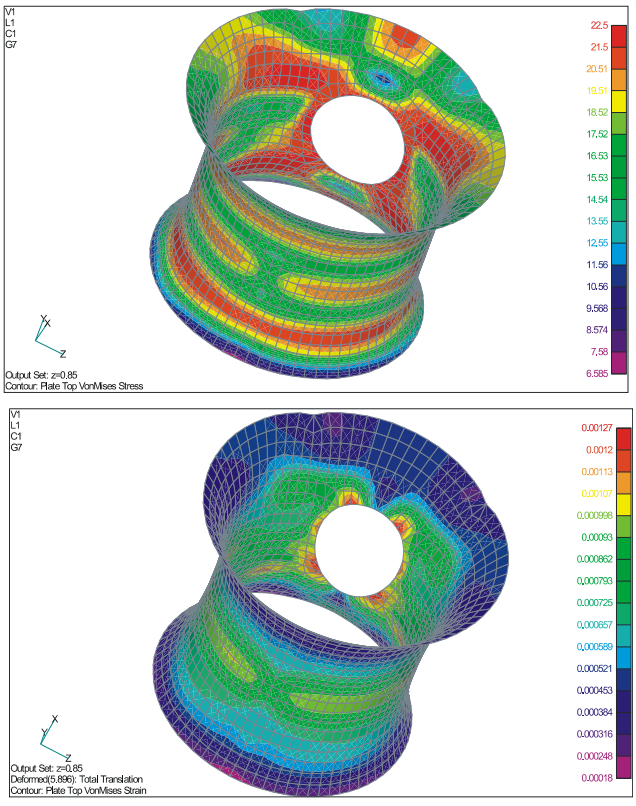

Figure 16. Distributions of the Von Misses stresses (up) and strains (down) on the cylindrical shell

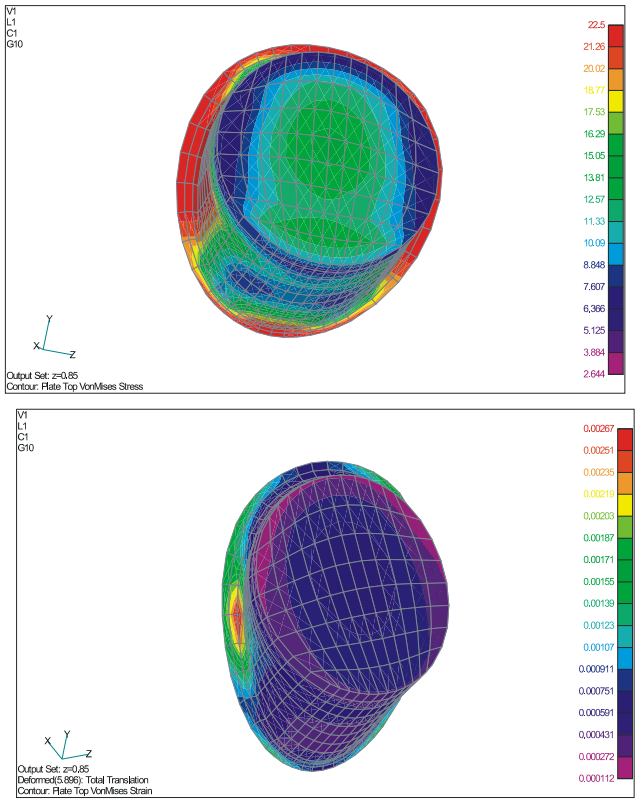

Figure 17. Distributions of the Von Misses stresses (up) and strains (down) on the toroidal container fitting with the cover

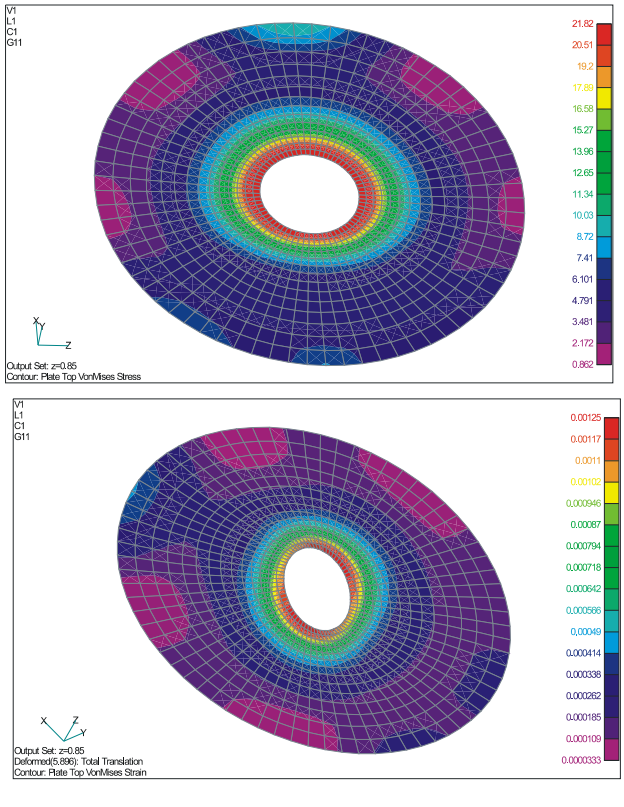

Figure 18. Distributions of the Von Misses stresses (up) and strains (down) on the marking plate

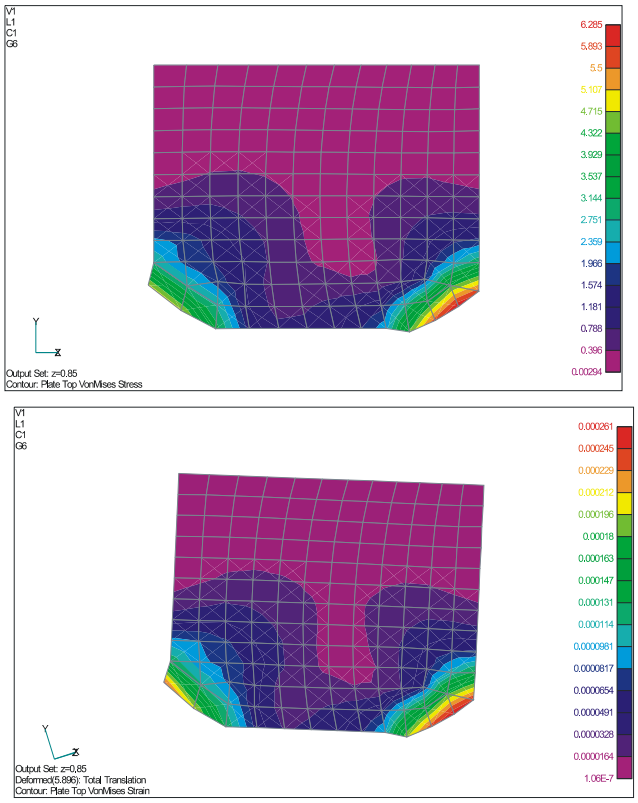

Figure 19. Distributions of the Von Misses stresses (up) and strains (down) on the barrier

Table 3. Maximum values of the Von Misses stresses and strains in the main parts of the container model for the test pressure

Pos.	Part name	Maximum value of Von Misses	
		Stress $\left(\mathrm{daN/mm^2}\right)$	Strain (%)
1	Top sphere	19.93	0.088
2	Bottom sphere	19.51	0.092
3	Cylindrical shell	22.50	0.127
4	Fitting with cover	22.50	0.267
5	Marking plate	21.82	0.125
6	Barrier	6.28	0.026

From Figures 14 to 19 as well as from Table 3, it can be seen that the maximum value of the Von Misses stress in the model is $\sigma_{VM} = 22.5\,\mathrm{daN/mm^2}$ and this value is somewhat lower than the allowable stress value $\sigma_y^c = 22.525\,\mathrm{daN/mm^2}$.

At the same time, it can be seen that the maximum Von Misses strain in the model is $\varepsilon_{VM} = 0.00267 = 0.267\%$. This value is lower than the allowable strain value $\varepsilon_y^c = 0.3186\%$.

These results demonstrate that all parts of the container satisfy technical requirements for the test pressure.

The structural analysis for the minimal allowable bursting pressure $p_b = 0.675\,\mathrm{daN/mm^2}$ was performed with the model which had the previously defined optimal shape of the cross section.

The distributions of the Von Misses stresses and strains in the main parts of the container model are shown in Figures 20 to 25 and their maximum values are given in Table 4.

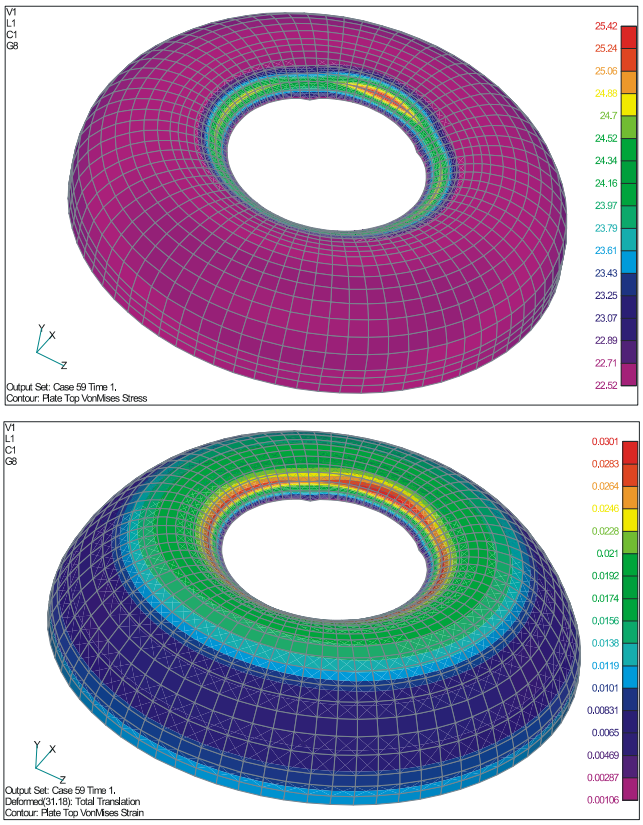

Figure 20. Distributions of the Von Misses stresses (up) and strains (down) on the top sphere

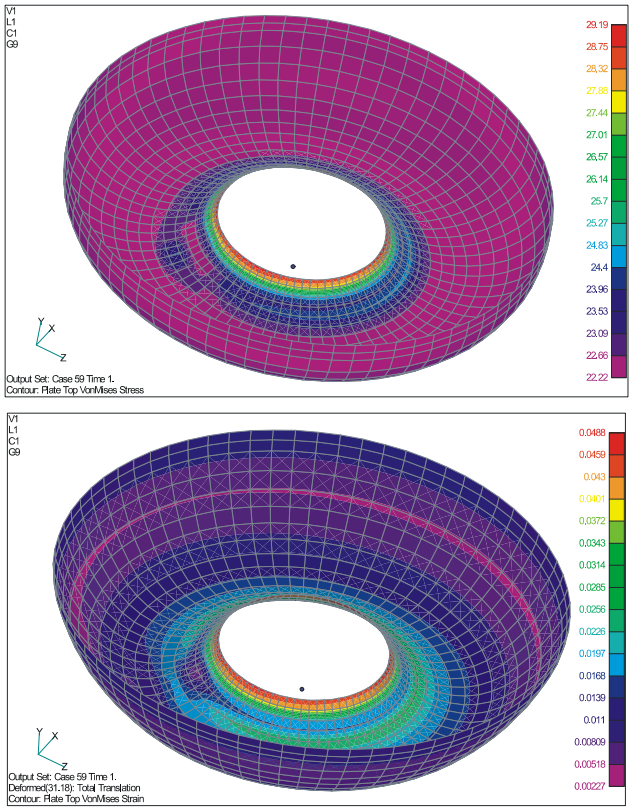

Figure 21. Distributions of the Von Misses stresses (left) and strains (down) on the bottom sphere

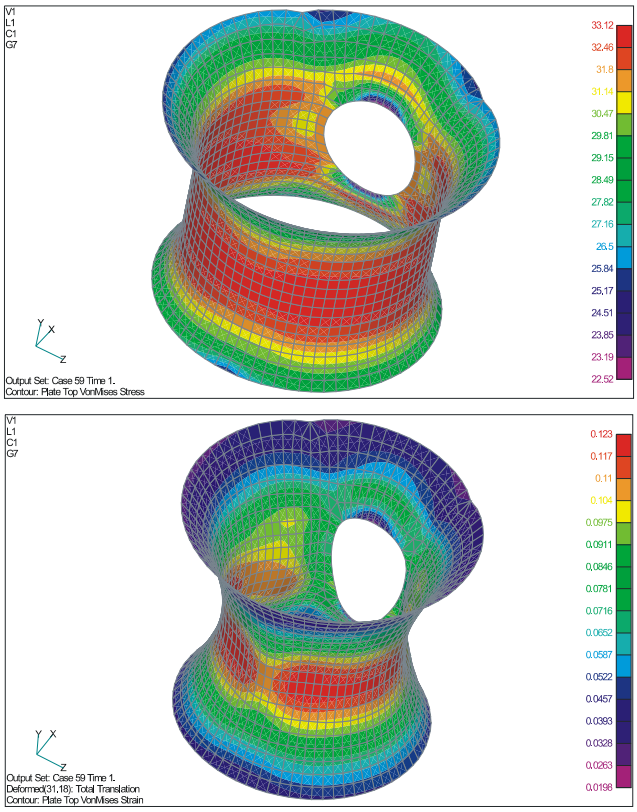

Figure 22. Distributions of the Von Misses stresses (up) and strains (down) on the cylindrical shell

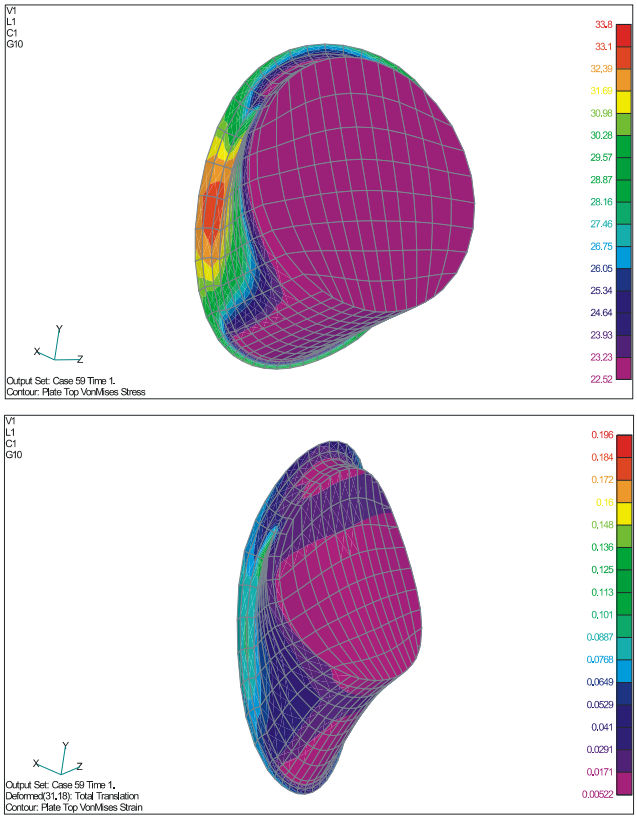

Figure 23. Distributions of the Von Misses stresses (up) and strains (down) on the fitting with the cover

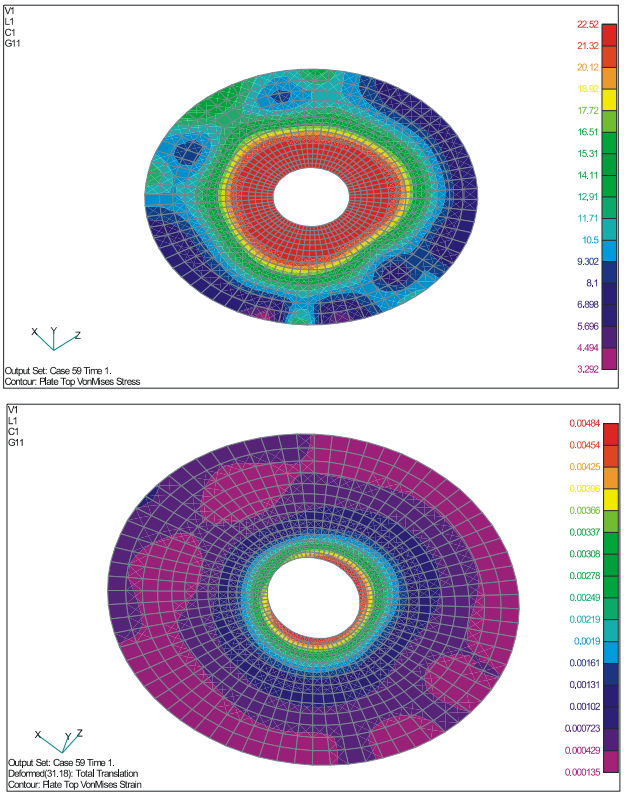

Figure 24. Distributions of the Von Misses stresses (up) and strains (down) on the marking plate

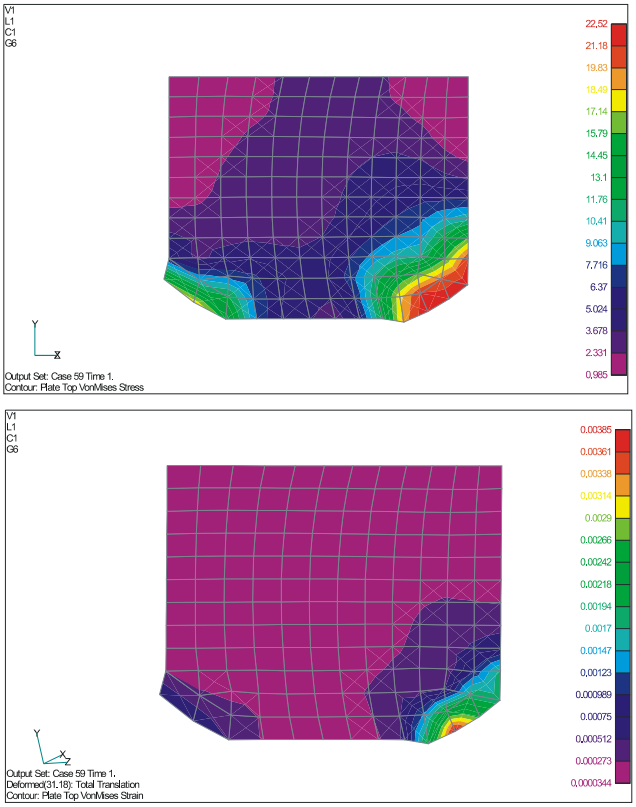

Figure 25. Distributions of the Von Misses stresses (up) and strains (down) on the barrier

Table 4. Maximum values of the Von Misses stresses and strains in the main parts of the container model for the bursting pressure

Pos.	Part name	Maximum value of Von Misses	
		stress $\left(\mathrm{daN/mm^2}\right)$	strain (%)
1	Top sphere	25.42	3.01
2	Bottom sphere	29.19	4.88
3	Cylindrical shell	33.12	12.3
4	Container fitting	33.8	19.6
5	Marking plate	22.52	0.48
6	Barrier	22.52	0.39

From Figures 20 to 25 as well as from Table 4, it can be seen that the maximum value of the Von Misses stress in the entire model is $\sigma_{VM} = 33.8\,\mathrm{daN/mm^2}$ that is a lower value than the allowable stress value $\sigma_m^c = 34.85\,\mathrm{daN/mm^2}$.

At the same time, it can be seen that the maximum Von Misses strain value in the entire model is $\varepsilon_{VM} = 0.196 = 19.6\%$. This value is considerably lower than the allowable strain value $\varepsilon_m = 28\%$.

These results demonstrate not only that container satisfies technical requirements for the bursting pressure, but also that the container could withstand a certain higher pressure level.

Concluding remarks

The complete computation procedure for the stress/strength analysis of the toroidal container for liquefied petroleum gas is presented.

It was not possible to use analytical methods for the calculation of the stress and strain state components of the LM-630toroidal container for liquefied petroleum gas and so the structural analysis was applied. The nonlinear structural analyses were used for that purpose.

The presented results of the structural analyses of the container confirm that the container satisfies all technical requirements in regard to the strength of container material.

It should be kept in mind that minimum values of the mechanical characteristics, additionally reduced, were used for the calculation. From this standpoint, it means that the analyses were somewhat conservative and on the safe side.

References

[1] VELIČKOVIĆ,V.: Stress concentration at points around elliptic opening in in-plane stressed multilayer orthotropic plate, Scientific Technical Review, 2002, Vol.LII, No.4, pp.37-43.

[2] VELIČKOVIĆ,V.: Contribution to analysis of stress state at points around elliptic opening in in-plane stressed orthotropic plate, Scientific Technical Review, 2007, Vol.LVII, No.1, pp.66-72.

[3] SUTCLIFFE,W.J,: Stress analysis of toroidal shells of elliptic cross-section, Int. J. Mech. Sci., 1971, 13, pp. 951-958.

[4] YAMADA,G., KOBAYASHI,Y., OHTA,Y., YOKOTA,S.: Free vibration of a toroidal shell with elliptical cross-section, J. Sound. Vibr., 1989, 135, 411-425.

[5] GALLETLY,G.D.: Elastic buckling of complete toroidal shells of elliptical cross-section subjected to uniform internal pressure, Thin-Walled Structures, 1998, 30, pp. 23-34.

[6] COMBESCURE,A. GALLETLY,G.D.: Plastic buckling of complete toroidal shells of elliptical cross-section subjected to internal pressure, Thin-Walled Structures, 1999, 34, pp. 135-146

[7] ECE Regulation No. 67 Revision 1

[8] VELIČKOVIĆ,V., BOJANIĆ,M., GREBOVIĆ,A.: Structural analysis of toroidal containers for liquefied petroleum gas (LPG), Minisymposia: Computational Methods in Structural Analysis and Optimization by FEM-within 1st ICSSM, Organizer: S. Maksimovic, Kopaonik 10th -13th April, 2007.

[9] TIMOSHENKO,S.P., WOINOWSKY – KRIGER,S.: *Theory of Plates and Shells*, McGRAW-HILL KOGAKUSHA, LTD., Japan, 1959

[10] JOSIFOVIĆ,M.: *Izabrana poglavlja iz elastičnosti i plastičnosti*, Mašinski fakultet, Beograd, 1970.

[11] ROARK, R. J. *Formulas for Stress and Strain*, McGraw-Hill Book Co., 1975.

[12] RAŠKOVIĆ,D.: *Teorija elastičnosti (Theory of elasticity)*, Naučna knjiga, Beograd 1986.

[13] MSC/NASTRAN Theoretical Manuals.

Received: 18.07.2007.

Stanja napona i deformacija u materijalu napregnutog toroidnog rezervoara za tečni naftni gas

Analitičke metode proračuna stanja napona i deformacija se sa zadovoljavajućom tačnošću mogu primeniti kod velikog broja tehničkih problema (videti, na primer, reference [1, 2])

Zbog netipičnog oblika preseka toroidnog rezervoara za tečni naftni gas LM-630, kao i postojanja izvora koncentracije napona, za proračun stanja napona deformacija u njegovim zidovima pod dejstvom unutrašnjeg pritiska, praktično je bilo nemoguće primeniti analitičke metode proračuna. Ove činjenice su bile razlog da se primeni strukturalna analiza.

U radu su, uz teorijska razmatranja, razmotreni najvažniji koraci kao i glavni rezultati numeričkog proračuna stanja napona i deformacija toroidnog rezervoara LM-630. Dobijeni rezultati pokazuju da rezervoar zadovoljava projektne zahteve u pogledu čvrstoće.

Ključne reči: **naponsko stanje, uticaj deformacije, strukturna analiza, toroidni rezervoar, tečni naftni gas.**

Etat de tension et déformations dans le matériel du réservoir toroïde pour le gaz liquéfié

Les méthodes analytiques pour le calcul de l'état de tension et déformations peuvent être appliquées avec exactitude satisfaisante pour un grand nombre de problèmes techniques (voir, par exemple, référence [1,2]). A cause de la forme non-typique de la section du réservoir toroïde pour le gaz liquéfié de pétrole LM- 630 et l'existence d'une source de concentration de la tension, il était pratiquement impossible d'appliquer les méthodes analytiques pour l'état de tension des déformations dans les parois, sous l'effet de la tension interne.Pour cette raison on a employé l'analyse structurale. Dans ce travail on a considéré aussi les plus importants pas ainsi que les principaux résultats du calcul numérique de l'état de tension et les déformations du réservoir toroïde LM-630. Les résultats obtenus démontrent que ce réservoir satisfait les exigences de solidité demandées par le projet.

Mots clés: **état de tension, déformation, effet de déformation, analyse structurale, réservoir toroïde, gaz de pétrole liquéfié**